J. CHEM. SOC. FARADAY TRANS., 1992, 88(19), 2805–2810

Dissociative Electron Attachment in Water and Methanol (5–14 eV)

Martin G. Curtis and Isobel C. Walker*
Department of Chemistry, Heriot-Watt University, Riccarton, Edinburgh EH14 4AS, Scotland, UK

Energies of D^- and O^- ions produced by dissociative electron attachment (DA) to D_2O and CD_3OD (and some partially deuteriated methanols) over three resonance regions (*ca.* 6.5, 8.5 and 10.5 eV) are reported. In both water and methanol over the first two resonances, the most probable D^- ion energy is close to the maximum possible, following rupture of the O—D bond to give ground-state products. Over the same two resonances in water, O^- ions appear to be produced in a symmetric dissociation accompanied initially by highly excited D_2 and, then, above the appropriate energy threshold, by D atoms. Dissociative pathways for the highest energy resonances are not established, but in methanol, the available experimental evidence points to dissociation from a relatively long-lived, rearranged complex (possibly $CD_2OD_2^-$). Attention is drawn, where comparison is possible, to similarities between the dissociative behaviour of anions (electron/molecule resonant states) and photodissociation of the parent neutral states.

The study of dissociative electron attachment (DA) to molecules [eqn. (i)]

$$e + AB \rightarrow [AB^-] \rightarrow A + B^- \quad \text{(i)}$$

offers information on short-lived molecular anions, or resonances ([AB^-], above) which complements that obtained from resonant electron scattering.[1] In addition, it provides insight into the dynamics of fast dissociation processes.[2] For the latter, measurement of the kinetic energy of the product negative ion is necessary.[3] Most recent work incorporating this has been reported by Illenberger, who inferred negative ion kinetic energies from differences in drift time of direct and turn-around ions through a quadrupole mass spectrometer, which doubled as a drift tube.[4] Others have used Wien filters[3] or conventional electrostatic devices for energy analysis.[2] The last mentioned are, in principle, most satisfactory, offering a direct measure of ion kinetic energy distributions. However, DA cross-sections are generally low, so that concomitant energy and mass analysis frequently reduces ion intensities to unacceptable levels. Consequently, few DA spectrometers routinely incorporate ion energy analysers. We have constructed a negative ion spectrometer in which the ions are energy analysed in a cylindrical mirror analyser prior to mass analysis in a quadrupole mass spectrometer. In this device, the signal intensity has been ameliorated by extracting ions from the collision region over an extended solid angle. In the present paper, we describe the spectrometer and report new DA data for water and methanol.

Dissociative electron attachment to water (H_2O) has been extensively studied.[2,5–14] with most effort directed at determination of resonance energies, identification of products and measurement of integral cross-sections; data obtained are summarized in ref. 13 and 14. Briefly, DA occurs for electrons of energy *ca.* 6.5, 8.8 and 11.8 eV,† respectively. Each DA process has been reported to yield H^-, O^- and OH^- ions, the last in very low yields. Schulz[9] established that, over the first two resonances (centred at 6.5 and 8.8 eV), dissociation is to $H^-(X\,^1S)$ and $OH(X\,^2\Pi)$, and the *maximum* kinetic energy release is the total available. Beliç *et al.* showed that the OH fragment appearing out of the lowest (6.5 eV) resonance carries some vibrational energy, while that from the 8.8 eV anion is primarily rotationally excited.[2] The angular distributions of the product H^- ions are compatible with resonances of symmetry $^2B_1$ (6.5 eV), $^2A_1$ (8.8 eV) and $^2B_2$ (11.8 eV).[2] Accordingly, they have been assigned to states comprising two $4a_1$ (3s, Rydberg) electrons bound to a positive ion core with a vacancy in the $1b_1$, $3a_1$ and $1b_2$ orbital, respectively.[2,14]

Methanol (CH_3OH), like water, undergoes three low-energy dissociative attachment processes centred, in this case, around 6.5, 8.0 and 10.5 eV.[10,15] CH_3O^- and H^- have been detected out of each of these. However, H^- energy analysis has not yet been reported. As this will carry away most of the kinetic energy released in a simple dissociation [*ca.* 97% for $(H + CH_3O)/(CH_3OH)$], kinetic energy measurements on the H^- moiety are important. Both OH^- (at near-thermal energies) and O^- (with *ca.* 1 eV kinetic energy) have been detected from the 10.5 eV resonance. In the case of OH^-, results from partially deuteriated methanols suggest that hydrogen scrambling precedes dissociation of the anion at 10.5 eV.[15]

Experimental

The spectrometer is illustrated diagrammatically in Fig. 1. Electrons from a tungsten filament travel through a seven-element electron gun to the collision region where target gas flows under single-collision conditions. Unscattered electrons pass through this region to a collector mounted at the centre of an end plate. An annulus, width 1 mm, mean radius 10 mm, is cut from this same end plate (Fig. 1, inset). Ions which diffuse to the annulus are extracted (over 360°) and directed to the entrance of a co-axial cylindrical mirror analyser (CMA); the ion-transfer optics are designed to launch the ions into the CMA at 42.3° with respect to the system axis, for second-order focussing. Energy-selected ions are finally mass analysed in a quadrupole mass spectrometer (QMA, Vacuum Generators SXP300) and detected on an off-axis Channeltron.

In the present series of experiments, the electron energy was set manually by adjustment of the collision region potential only; with a small applied axial magnetic field ($< 15 \times 10^{-4}$ T), electrons of energy down to *ca.* 2 eV were usable. The QMA was tuned to the target ion and the CMA set to transmit ions of energy 20 eV, at which the resolution was *ca.* 1 eV. The ion energy was scanned, under computer control, over a chosen range and data accumulated as required. The electron energy was then changed manually and the ion energy scan repeated.

When the QMA was tuned to transmit H^- ions, some scattered electrons reached the detector. This problem did not arise with D^- and so the present experiments were carried out mainly on deuteriated species.

† 1 eV ≈ 1.602×10^{-19} J.

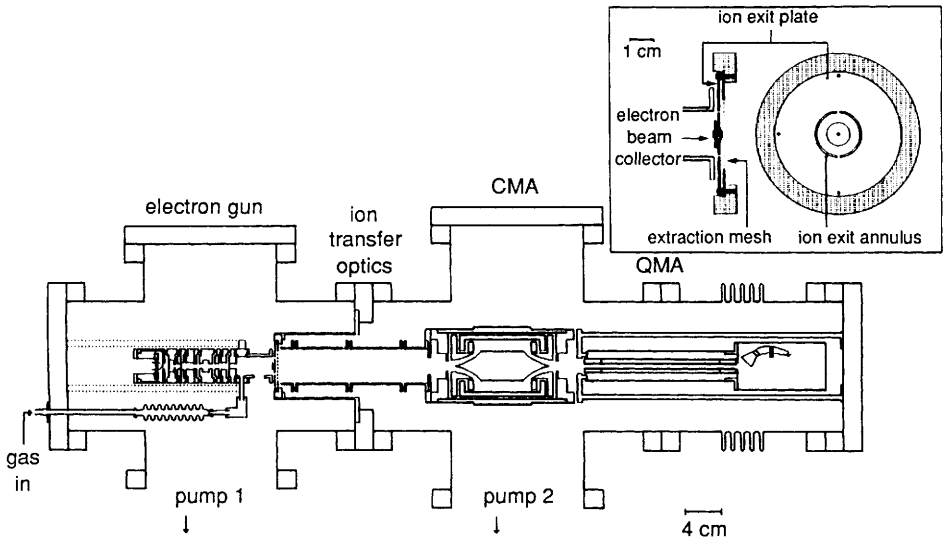

Fig. 1 Diagram of the apparatus with (inset) detail of the ion extraction region

Both the electron- and ion-energy axes were calibrated from the O^-/O_2 reaction (see below).

Results

The DA cross-section for O^-/O_2 is established.[16] Its maximum value is at 6.5 eV incident electron energy; the threshold energy is 3.7 eV[17] and excess energy above this threshold is shared equally between the two (ground-state) products. We use this reaction for energy calibration, as illustrated in Fig. 2. Thus, Fig. 2(*a*) displays the O^- signal as a function of ion energy, at a fixed incident electron energy. The width of this distribution curve is set by the CMA resolution. Fig. 2(*b*) was constructed from a series of such distribution curves. It shows the *maximum* recorded signal *vs.* incident electron energy, and traces out the DA cross-section; agreement with the known cross-section is excellent.[16] This curve is used to calibrate the electron energy axis (E_{max} = 6.5 eV). In Fig. 2(*c*), the most probable ion energy is plotted against electron energy. The best straight line through the experimental points has gradient 0.50, as required by the equipartition of the excess energy between the two fragments. The ion energy axis is calibrated by setting zero at the dissociation threshold (3.7 eV).

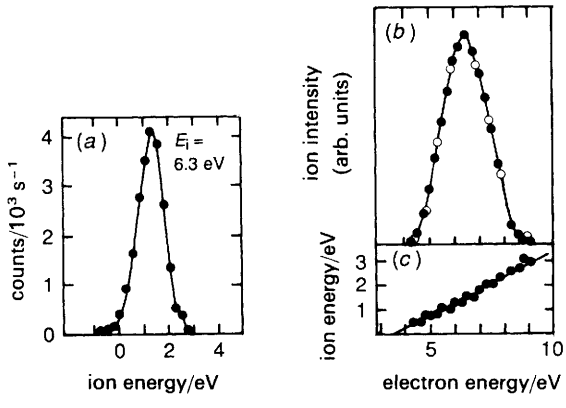

Fig. 2 O^-/O_2 (*a*) ion energy distribution at an incident electron energy (E_i) of 6.3 eV; (*b*) maximum ion signal as a function of incident electron energy: (●) present results, (○) data points taken from ref. 16 and normalised at the maximum; (*c*) most probable ion energy as a function of incident electron energy. The line through the data points has gradient 0.50. These results were used to calibrate electron and ion energies

These data confirm, also, that over an ion energy range of at least 3 eV, the ion detection efficiency does not vary with ion energy.

For reasons given above, measurements were made mostly on deuteriated molecules. Results for water are contained in Fig. 3 (D^-/D_2O) and Fig. 4 (O^-/D_2O). In Fig. 5, total cross-sections for production of D^- and O^- are shown along with an optical absorption spectrum for water, recorded by us (at the SRS source, Daresbury[18]) and presented here on an energy (eV) axis to allow direct comparison with the DA results.

Data for CD_3OD (D^- and O^-) are contained in Fig. 6 and 7. The material in Fig. 7 refers to partially deuteriated methanols, recorded in order to identify the originating site of the D^- ions. In Fig. 8 DA results for methanol are compared with an optical spectrum and a near-threshold electron energy-loss spectrum, both recorded by us, using experimental methods previously described.[18]

In D_2O, the OD^- signal was too low for energy analysis. In methanol, we could not detect measurable levels of OD^- or CD_3O^-.

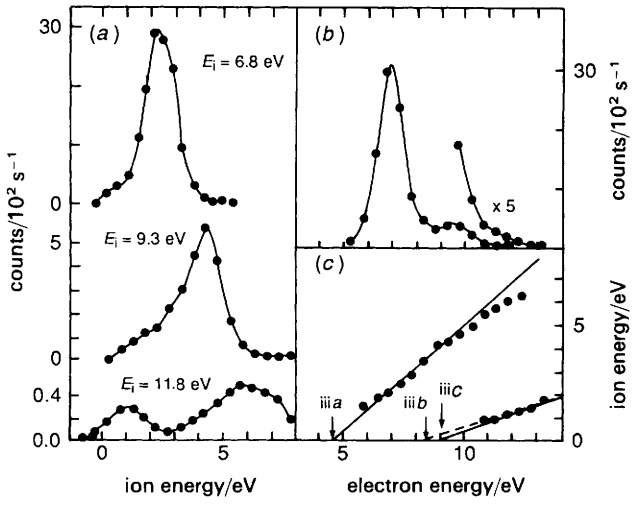

Fig. 3 D^-/D_2O (*a*) ion energy distributions at the stated electron energies; (*b*) maximum ion signal *vs.* electron energy; (*c*) most probable ion energy *vs.* electron energy. Energy thresholds of some processes (labelled according to equation numbers) are indicated. The solid lines are the maximum possible ion kinetic energies. The broken line has gradient 0.36

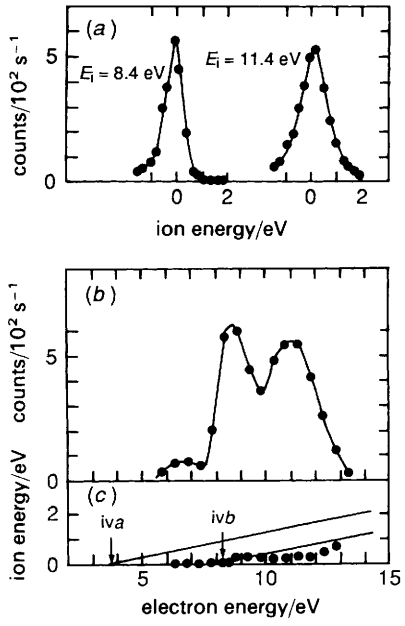

Fig. 4 O^-/D_2O (*a*) Ion energy distributions at the stated electron energies; (*b*) maximum ion signal *vs.* electron energy; (*c*) most probable ion energy *vs.* electron energy. Solid lines are maximum possible ion kinetic energies for the processes labelled [eqn. (iv)]

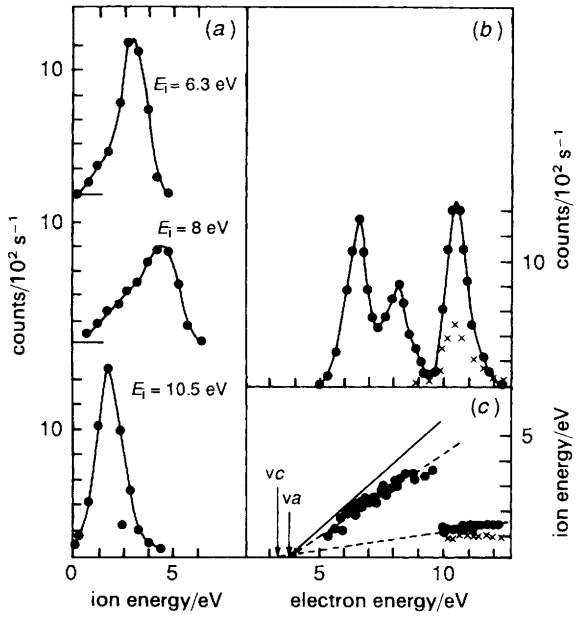

Fig. 6 D^-, O^-/CD_3OD (*a*) D^- ion energy distributions at the stated electron energies; (*b*) (●) D^- and (×) O^- signal *vs.* electron energy; (*c*) (●) D^- and (×) O^- ion energies *vs.* electron energy. The solid line is maximum possible kinetic energy. Broken lines have gradients 0.72 and 0.18, respectively

We cannot evaluate absolute cross-sections. However, all the reported signals (counts) were recorded under comparable conditions, so that relative cross-sections may be roughly estimated from these.

Discussion

Water

The electron configuration of water (C_{2v} symmetry) is $(1a_1)^2(2a_1)^2(1b_2)^2(3a_1)^2(1b_1)^2$. The lowest electronically excited states are all of Rydberg character,[19,20] the first of these, the optical A state being $^1B_1$ ($1b_1$ 3s); it presents a broad structureless band ($E_{max} \approx 7.4$ eV) in the VUV absorption spectrum (Fig. 5). The optical B state, which also gives a broad VUV band ($E_{max} \approx 9.7$ eV, Fig. 5), is $^1A_1$ ($3a_1$ 3s). Excitation of the C state ($^1B_1$, $1p_1$ $3p_z$, origin 10.00 eV) leads to typically sharp, Rydberg bands; likewise for the D state ($^1A_1$, $1b_1$ $3p_x$, origin 10.17 eV). The third $1b_1$ 3p component ($^1A_2$, $1b_1$ $3p_y$) is electric-dipole forbidden, but is thought to have been detected at 9.1 eV in electron energy-loss (EEL) spectra.[21] In all cases singlet–triplet splittings are small; energies of some triplet states, taken from EEL spectra,[21] are included in Fig. 5. These states are relevant to the identification of the anionic states detected in the DA work.

A species, mass *m*, produced by dissociation of a molecule, mass *M*, into two fragments carries kinetic energy *W* given by:

$$W = (1 - m/M)E_T \qquad \text{(ii)}$$

where E_T is the total translational energy of the two dissociation products. In the case of D^-/D_2O this becomes $W_{D^-} = 0.9E_T$, while for O^-/D_2O, $W_{O^-} = 0.2E_T$. For disso-

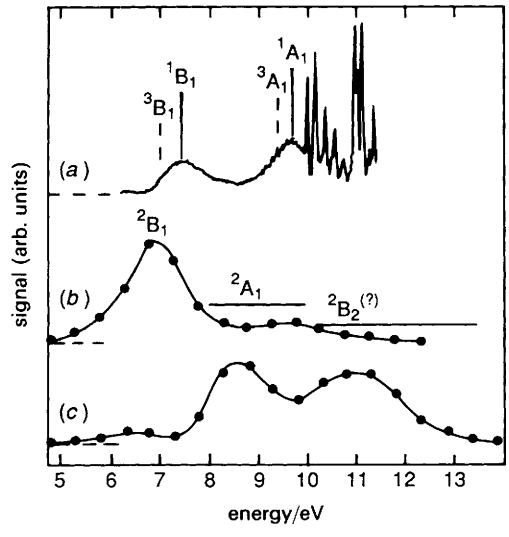

Fig. 5 Water–DA cross-sections (D_2O) compared with a VUV spectrum (H_2O), showing the relation of proposed resonant states to parent states. Positions of triplet states are taken from ref. 21. (*a*) VUV; (*b*) D^-/D_2O; (*c*) O^-/D_2O

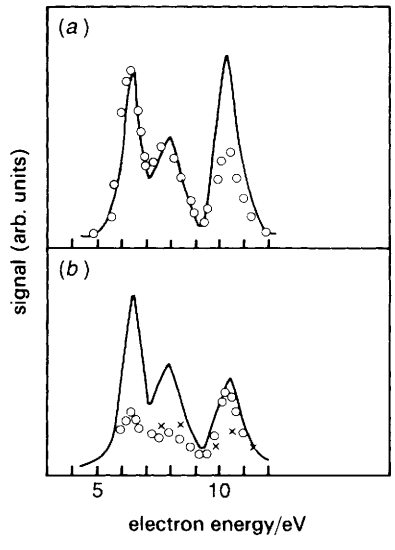

Fig. 7 (*a*) (—) D^-/CD_3OD and (○) D^-/CH_3OD, normalised at the first maximum; (*b*) (—) D^-/CH_3OD, (○) D^-/CD_3OH and (×) D^-/CH_3OH

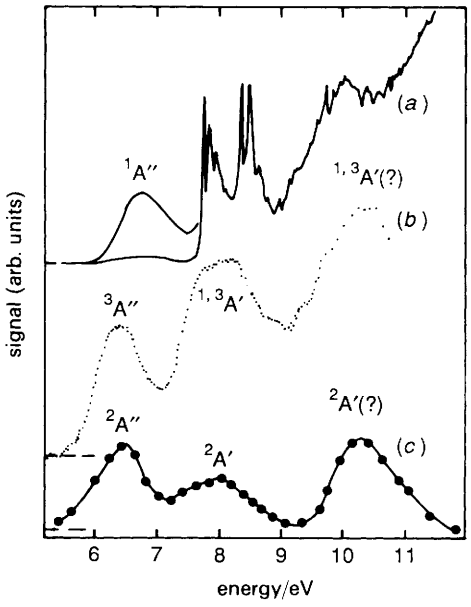

Fig. 8 Methanol–DA cross-sections (CD_3OD) compared with VUV (CH_3OH) and EEL (CH_3OH) spectra, showing the relation of proposed resonant states to parent states: (*a*) VUV; (*b*) EEL; (*c*) D^-/CD_3OD

ciation into more than two species, it is not generally possible to describe the kinetic energy partitioning from the translational energy of a single fragment. However, if the dissociation is symmetric, as could happen in D_2O, with a D_2 group retreating from O, and subsequently dissociating to D + D (with identical kinetic energies), then the problem reduces to a two-body one and the kinetic energy partitioning is D : D : O = 0.4 : 0.4 : 0.2. That is, for fragmentation of D_2O along such a symmetric pathway, $W_{D^-} = 0.4\ E_T$ and $W_{O^-} = 0.2\ E_T$.

Relevant reactions leading to D^-/D_2O and O^-/D_2O and their threshold energies[17] are:

$$D^- + OD(X\,^2\Pi); \quad 4.52\ eV \qquad (iii\textit{a})$$

$$D_2O + e \rightarrow D^- + OD(A\,^2\Sigma); \quad 8.38\ eV \qquad (iii\textit{b})$$

$$D^- + D + O; \quad 9.02\ eV \qquad (iii\textit{c})$$

$$D_2O + e \rightarrow \begin{cases} O^- + D_2; & 3.68\ eV \qquad (iv\textit{a}) \\ O^- + D + D; & 8.28\ eV \qquad (iv\textit{b}) \end{cases}$$

From eqn. (ii), the maximum possible kinetic energy of an ion formed in a simple dissociation is $W_{max} = (1 - m/M)(E_i - E_{thr})$, where E_i is the incident electron energy and E_{thr} the energy threshold. Maximum possible energies for the above reactions are included in Fig. 3(*c*) and 4(*c*) as the solid lines.

We discuss the experimental data in three regions corresponding to previously observed resonant processes.

Region I, ca. 6.5 eV

The lowest resonance is visible in both the D^- and O^- cross-sections [Fig. 3(*b*), 4(*b*)].

The present data for D^- energies over the resonance are in accord with previous work.[2,9] Specifically, the most probable (as opposed to the maximum[9]) ion energy is close to the maximum available following dissociation to D^- (^1S) + OD ($X\,^2\Pi$) [Fig. 3(*c*)]. Low-energy tails in the ion energy distribution curves arise from vibrational excitation of the OD [Fig. 3(*a*)], as previously demonstrated.[2]

For O^- production in the first resonance region, the only energetically possible reaction is (iv*a*), where the dissociation partner is D_2. In this case, if the initial attachment is vertical, then, at the birth of the anion, the D–D internuclear distance (taken as that in the ground state neutral) is *ca.* 150 pm, while the equilibrium bond length in D_2 is 74 pm; accordingly, the D_2 molecule which separates from the O^- must be highly vibrationally excited. Consistent with this, the O^- kinetic energy does not exceed thermal values [Fig. 4(*c*)].

The lowest DA process in water now seems to be well characterised. There are two major dissociation channels. The more probable of these is a rapid bond rupture leading (in D_2O) to D^-, which accommodates most of the available energy, together with vibrationally excited OD. The second channel leads to O^-, having near-thermal energies, accompanied by highly excited D_2. The accepted assignment for the participating resonance, $^2B_1$,[2,14] fits with all the available experimental evidence. The so-called parent of the resonant (anionic) state is the optical $^{1,3}B_1$ state (Fig. 5). Photodissociation of the parent singlet component has been thoroughly investigated by both theory and experiment.[22] In this, rupture of the OH bond (the only observed photodissociation pathway) leads to ground-state products which carry away most of the excess energy as kinetic energy. There is some vibrational excitation of the OH fragment, but rotational excitation is very weak. As described above, this behaviour is mimicked by the dissociating $^2B_1$ resonance. It therefore seems likely that the potential-energy surface (PES) established for the $^1B_1$ state[23] (a surface which is dissociative along the O—H coordinate in the Franck–Condon region and isotropic near the ground-state equilibrium angle) could be adapted to the $^2B_1$ resonance.

Region II, ca. 9 eV

The D^- energy over this resonance (Fig. 3) shows conclusively that the dissociation partner is OD ($X\,^2\Pi$).[9] The most probable energy is slightly less than the maximum available; we know from previous work that the accompanying OD is rotationally excited.[2] This behaviour parallels that observed in photodissociation of the $B\,^1A_1$ state of the neutral molecule.[24] Thus, photodissociation of the B state of H_2O leads mainly to H and OH ($X\,^2\Pi$), the latter rotationally excited.[25,26] The rotational excitation originates in an anisotropic potential which causes the bond angle to open in the early stages of the dissociation.[27] The second resonance in water has been assigned $^2A_1$, daughter of this optical A_1 state.[2,14] The above comments on the product energies are consistent with this assignment, with the additional implication that the potential-energy surfaces of the $^2A_1$ and $^1A_1$ states are alike. However, the $^1A_1$ state of water correlates with H + OH($A\,^2\Sigma$); the ground-state OH ($X\,^2\Pi$), the major product of photodissociation, arises from predissociation by the $A\,^1B_1$ state.[27] If a parallel correlation holds for the $^2A_1$ anion [namely, here, D^- + OD($A\,^2\Sigma$)], the $^2A_1$ must be predissociated by the $^2B_1$ state to give ground-state OD.

In the O^- channel, the energy threshold for fragmentation [reaction (iv*b*)] falls within the second resonance; at that point, there is a slight rise in the kinetic energy of the negative ion [Fig. 4(*c*)]. The energy increase is close to that expected for a symmetric double dissociation, as discussed above. In this picture, the internal energy of the accompanying D_2 increases smoothly to the dissociation limit, at which point the departing D atoms (which have equal kinetic energies) impart momentum to the O^-.

Region III, ca. 11.5 eV

The third resonance is obvious in the O^- [Fig. 4(*b*)] but not the D^- [Fig. 3(*b*)] cross-section. However, as the incident electron energy is increased through region II, energetic D^- ions (see above) are joined by low-energy ones. Without ion energy analysis, the low-energy D^- ions would not be

detected.[2] We assume that the high-energy ions are from resonance II and the low-energy ones from resonance III.

For the production of the low-energy D^- ions, we discount process (iii*a*) because the energy remaining in the OD would be much greater than the bond dissociation energy. The energy data (Fig. 3) would suit a symmetric fragmentation with the excess energy partitioned $D^- : D : O = 0.4 : 0.4 : 0.2$ [reaction (iii*c*)]. Equally, the measured ion energies could accommodate reaction (iii*b*), provided that only *ca.* 40% of the total available excess energy is released as kinetic energy of the D^- and OD ($^2\Sigma$). However, under these circumstances, the vibrationally/rotationally excited OD would probably predissociate[28] so that the end result would be fragmentation. An alternative, asymmetric, fragmentation would require initial separation of OD^- from D with close dissociation of the OD^- to $D^- + O$. We introduce this last possibility because the O^- energies over most of the energy range are lower than expected for a symmetric double dissociation [Fig. 4(*c*)], and an asymmetric fragmentation must be considered in this case.

This third resonance has been assigned to a single anionic state, $^2B_2$ $[(1b_2)^1\ (4a_1)^2]$, parent $^{1,3}B_2$ $[(1b_2)^1\ (4a_1)^1]$.[2,14] The proposed parent state has not, so far, been located. Tentative experimental values, from EEL, are 11.3 eV for the triplet and 11.7 eV for the singlet.[21] However, from ionisation energy differences,[29] the singlet is expected to lie *ca.* 3 eV above the optical B state, *i.e.* in the region of 12.5 eV, which would be more suited to the DA data. This picture of one dissociating state is pleasing in its simplicity and in its relationship to the likely lower-lying negative ions. However, the resonance covers a congested spectral region (Fig. 5) which contains structure Rydberg states that are known to support relatively long-lived Feshbach resonances[30] and which may be implicated in DA.

Methanol

The electron configuration of methanol (C_s symmetry) is $\ldots(6a')^2(7a')^2(2a'')^2$. As for water, the low-lying excited electronic states are all of Rydberg-type.[19,20] Of these, the optical A state is $^1A''$, 2a″ 3s (Fig. 8). The $^1A'$ (7a′ 3s) state, corresponding to the B ($^1A_1$) state of water, has not been identified from optical spectroscopy. We believe it (along with the associated triplet state) to be responsible for most of the signal around 8 eV in near-threshold EEL spectra (Fig. 8). The lowest triplet state a^3A'' (2a″ 3s) is also strongly excited on impact with electrons of low energy. We position it at 6.5 eV, *ca.* 0.3 eV below the singlet ($A^1\ A''$), in agreement with a previous estimate.[31]

Dissociative processes of relevance here and their energy thresholds[17] are:

$$CH_3OH + e \rightarrow \begin{cases} H^- + CH_3O; & 3.75\ eV & (va) \\ CH_3O^- + H; & 2.97\ eV & (vb) \\ H^- + CH_2OH; & 3.34\ eV & (vc) \\ H^- + CH_3 + O; & 7.71\ eV & (vd) \\ H^- + CH_2 + OH; & 8.1\ eV & (ve) \\ H^- + H + CH_2O; & 4.65\ eV & (vf) \end{cases}$$

$$CH_3OH + e \rightarrow \begin{cases} O^- + CH_4; & 2.39\ eV & (via) \\ O^- + CH_3 + H; & 7.01\ eV & (vib) \\ O^- + CH_2 + H_2; & 7.24\ eV & (vic) \end{cases}$$

Differences between the listed threshold energies and those applicable to the deuteriated compounds are not significant, within the resolution of the present measurements.

For $(D^- + CD_3O)/CD_3OD$, $W_{D^-} = 0.94E_T$ and for $(O^- + CD_4)/CD_3OD$, $W_{O^-} = 0.55E_T$ [eqn. (ii)].

Comparison of the D^- yields from CD_3OD and CH_3OD [Fig. 7(*a*)] show that, over the first two resonances, the D^- ions come from the OD group, but over the highest energy resonance some ions must originate in the methyl group. This is confirmed from CD_3OH data [Fig. 7(*b*)]. In this case, the D^- signal is recorded over all the resonances. However, results with the instrument tuned to collect D^- from CH_3OH demonstrated that from 5 to 9 eV this signal resulted from collection of H^- ions [Fig. 7(*b*)]. That is, taken together, these results show the D^- ions to come from the OD group at 5–9 eV, but from both hydroxy and methyl groups around 10.5 eV.

Regions I and II, ca. 6.5 and 8 eV

We detect only D^- out of the two lowest resonances. The ion energy increases relatively smoothly across the two resonant states. As indicated above, results for partially deuteriated methanols (Fig. 7) show the D^- to come exclusively from the OD group. The energy measurements are consistent with rapid rupture of the O—D bond to give D^- (^1S) + CD_3O ($\tilde{X}\ ^2E$) with, on average, *ca.* 75% of the available excess energy appearing as translational energy of the two products. Internal energy losses are slightly higher for the second (8 eV) process, as seen in both the ion energy data [Fig. 6(*c*)] and the (broadened) ion energy distribution curves [Fig. 6(*a*)]. Thus, in the D^- channel, these two dissociations closely resemble the corresponding processes in water.

There can be little doubt, given its energy, and by analogy with water, that the lowest resonant state is a Feshbach (two particle, one-hole) resonance, $^2A''$ $[(2a'')^1\ (3s)^2]$ whose parent is the $^{1,3}A''$ (2a″ 3s) state (Fig. 8). Studies on the photodissociation of the parent singlet state have recently been reported;[32] interestingly, they show it to proceed by rapid dissociation of the O—H (O—D) bond, and the energy partitioning (translational : internal) matches that observed here. In this, also, the similarity to water is maintained.

The nature of the second resonance is less easily established from available experimental data, because it spans several, structured Rydberg states (Fig. 8) which almost certainly support Feshbach resonances. However, given the simplicity of the observed DA processes, and again by analogy with water, we propose $^2A'$ $[(7a')^1\ (3s)^2]$, the Feshbach resonance whose parent is $^{1,3}A'$ (7a′ 3s), located *ca.* 8 eV in near-threshold EEL (Fig. 8).

Region III, ca. 10.5 eV

The most probable energy of the D^- ions out of the third resonance increases only very slightly, if at all, over the range of the resonance. This suggests an 'attractive' PES, which allows time for efficient redistribution of energy through the anion, prior to dissociation.[33,34] Further, the D^- ions originate in both the hydroxy and the methyl groups (Fig. 7 and above) although the D^- energy distribution is relatively sharp [Fig. 6(*a*)]. We therefore suppose that the D^- ions leave from equivalent sites in a relatively long-lived, rearranged complex, possibly $[CD_2OD_2]^-$. Such a rearranged intermediate would also account for the appearance of both OH^- and OD^- from partially deuteriated methanols.[15] As indicated previously, we did not detect any hydroxyl ions. Neither could we pick up CD_3O^- (or CH_3O^-/CH_3OH). Their observation in an earlier study shows that a rapid dissociation, with O—H bond rupture, also happens.[15]

Like the D^-, the O^- ion energy is, within the limits of the experimental measurements, constant at *ca.* 1 eV over the resonance, as has been previously reported.[15] We cannot, identify the dissociation pathway. If the O^- comes from the

rearranged species, $CD_2OD_2^-$, then the reaction is probably (*vic*), although, at the other extreme, we cannot exclude (*via*) with vibrationally/rotationally excited methane, which probably then dissociates.

On a simplistic view, and by analogy with water, a possible electron configuration contributing to this 10.5 eV resonance is $2A'$ $[(6a')^1\ (3s)^2]$. From ionisation energy differences,[29] the parent $^1A'$ state is expected around 11.0 eV, close to the first ionisation energy.

Conclusions

Dissociative electron attachment reactions in water and methanol are similar. Thus, in each, below *ca.* 12 eV, there are three resonant processes. For the first two of these, the available experimental data support assignments to two-particle, one-hole species, in which the particles (electrons) are in 3s Rydberg orbitals and the hole is in the HOMO and HOMO-1, respectively. Rapid dissociation of these anions provides increasingly energetic hydride ions, as the incident electron energy is increased by 5–6 eV, in each species. In contrast, the highest resonances produce ions of relative low energies; in methanol, the evidence points to the existence of a relatively long-lived, rearranged complex around 10.5 eV.

Where comparisons are possible (namely for two states in water and one in methanol), dissociative behaviour of an anion parallels that of photodissociation of the parent, suggesting similar potential-energy surfaces for parent molecule and daughter anion. This is an extension of the known similarity of the potential-energy surfaces of Rydberg-excited states and corresponding cations (one-hole states). A consequence of this last phenomenon is that the profile of an ionisation band in a photoelectron spectrum is reproduced in optical absorption bands of Rydberg states with that ionic core; this is widely used in the assignment of Rydberg bands in electronic spectra.[18] It may now be possible, for water at least, to adapt known potential-energy surfaces of the neutral to further our understanding of the dynamics of the dissociative attachment reactions. Conversely, if electrons can be used to probe extended regions of a PES and so access different dissociation pathways (as here), transfer of information from DA to photodissociation may be fruitful.

We are grateful to Mr. W. Stirling for technical assistance, to Mr. D. F. Dance who collaborated at the planning and design stages of the experiment, to Dr. J. Woolsey for material contributions and advice, and to Dr. M. A. D. Fluendy for helpful discussions. The work was supported by the SERC through a Research Grant (GR/E35916) and a studentship (to M.G.C.).

References

1 M. Allan, *J. Electron Spectrosc. Relat. Phenom.*, 1989, **48**, 219.
2 D. S. Belic, M. Landau and R. I. Hall, *J. Phys. B: At. Mol. Phys.*, 1981, **14**, 175.
3 P. J. Chantry, *Phys. Rev.*, 1968, **172**, 125.
4 E. Illenberger, *Ber. Bunsenges. Phys. Chem.*, 1982, **86**, 252.
5 W. W. Lozier, *Phys. Rev.*, 1930, **36**, 1417.
6 M. M. Mann, A. A. Hustrulid and I. T. Tate, *Phys. Rev.* 1940, **58**, 340.
7 I. S. Buchel'nokova, *Soviet Phys. JETP*, 1959, **8**, 783.
8 M. Cottin, *J. Chim. Phys.*, 1959, **56**, 1024.
9 G. J. Schulz, *J. Chem. Phys.*, 1960, **33**, 1661.
10 L. von Trepka and H. Neuert, *Z. Naturforsch., Teil A*, 1963, **18**, 1295.
11 F. H. Dorman, *J. Chem. Phys.*, 1966, **44**, 3856.
12 R. N. Compton and L. G. Christophorou, *Phys. Rev.*, 1967, **154**, 110.
13 C. E. Melton, *J. Chem. Phys.*, 1972, **57**, 4218.
14 M. Jungen, J. Vogt and V. Staemmler, *Chem. Phys.*, 1979, **37**, 49.
15 A. Kuhn, H-P. F. Fenzlaff and E. Illenberger, *J. Chem. Phys.*, 1988, **88**, 7453.
16 P. J. Chantry and G. J. Schulz, *Phys. Rev.*, 1967, **156**, 134.
17 H. M. Rosenstock, K. Draxl, B. W. Steiner and J. T. Herron, *J. Phys. Chem. Ref. Data*, 1977, 6.
18 I. C. Walker, M. H. Palmer and A. Hopkirk *Chem. Phys.*, 1989, **141**, 365.
19 W. R. Wadt and W. A. Goddard III, *Chem. Phys.*, 1976, **91**, 1.
20 M. B. Robin, *Higher Excited States of Polyatomic Molecules*, Academic Press, New York, 1974, vol. I; 1975, vol. II.
21 A. Chutjian, R. I. Hall and S. Trajmar, *J. Chem. Phys.*, 1975, **63**, 892.
22 P. Andresen and R. Schinke, in *Molecular Photodissociation Dynamics*, ed. M. N. R. Ashfold and J. E. Baggott, Royal Society of Chemistry, London, 1987.
23 V. Staemmler and A. Palma, *Chem. Phys.*, 1985, **93**, 63.
24 T. Carrington, *J. Chem. Phys.*, 1964, **41**, 2012.
25 H. J. Krautwald, L. Schneider, K. H. Welge and M. N. R. Ashfold, *Faraday Discuss. Chem. Soc.*, 1986, **82**, 99.
26 K. Weide and R. Schinke, *J. Chem. Phys.*, 1989, **90**, 7105.
27 J. P. Vinogradov and F. Vilesov, *Opt. Spectrosc.*, 1976, **40**, 32.
28 E. F. Van Dishoeck and A. Dalgarno, *J. Chem. Phys.*, 1983, **79**, 873.
29 K. Kimura, S. Katsumala, Y. Achiba, T. Yamazaki and S. Iwata, *Handbook of* He I *Photoelectron Spectra of Polyatomic Molecules*, Japan Sci. Soc. Press, Tokyo, 1977.
30 L. Sanche and G. J. Schulz, *J. Chem. Phys.*, 1973, **58**, 479.
31 F. W. E. Knoop, H. H. Brongersma and L. J. Oosterhoff, *Chem. Phys. Lett.*, 1972, **13**, 20.
32 S. Satyapal, J. Park and R. Bersohn, *J. Chem. Phys.*, 1989, **91**, 6873.
33 S. Goursand, M. Sizun and F. Fiquet-Fayard, *J. Chem. Phys.*, 1976, **65**, 5453.
34 S. Goursand, M. Sizun and F. Fiquet-Fayard, *J. Chem. Phys.*, 1978, **68**, 4130.

Paper 2/02892A; *Received 2nd June*, 1992